Alexandria Engineering Journal (2023) 69, 383–402

HOSTED BY

Alexandria University

Alexandria Engineering Journal

www.elsevier.com/locate/aej
www.sciencedirect.com

ORIGINAL ARTICLE

Numerical investigation of the effect of the turbulator geometry (disturber) on heat transfer in a channel with a square section

As'ad Alizadeh [a], Azher M. Abed [b], Hussein Zekri [c,h], Ghassan Fadhil Smaisim [d,e], Bahram Jalili [f], Pooya Pasha [g,i,*], Davood Domiri Ganji [g]

[a] *Department of Civil Engineering, College of Engineering, Cihan University-Erbil, Erbil, Iraq*
[b] *Air Conditioning and Refrigeration Techniques Engineering Department, Al-Mustaqbal University College, Babylon 51001, Babylon, Iraq*
[c] *Department of Mechanical Engineering, College of Engineering, University of Zakho, Zakho, Kurdistan Region, Iraq*
[d] *Department of Mechanical Engineering, Faculty of Engineering, University of Kufa, Iraq*
[e] *Nanotechnology and Advanced Materials Research Unit (NAMRU), Faculty of Engineering, University of Kufa, Iraq*
[f] *Department of Mechanical Engineering, Faculty of Engineering, North Tehran Branch, Islamic Azad University, Tehran, Iran*
[g] *Department of Mechanical Engineering, Noshirvani University of Technology, Babol, Iran*
[h] *College of Engineering, The American University of Kurdistan, Duhok, Kurdistan Region-Iraq*
[i] *Department of mechanical engineering, Mazandaran university of science and technology, Babol, Iran*

Received 12 November 2022; revised 19 January 2023; accepted 4 February 2023
Available online 15 February 2023

KEYWORDS

Finite volume method;
Heat transfer;
Nusselt number;
Reynolds number;
Turbulent flow

Abstract The principal moot point in this investigation is heat removal from surfaces with high heat flux, which is the use of tabulators and parts with a particular geometry, it has been chosen as a solution to this moot point. The primary hypothesis in this investigation is to increase fluid heat transfer by increasing turbulence and heat transfer by increasing the plane of heat transfer and establishing a vortex flow. The fundamental idea and novelty of this investigation is the simultaneous use of a turbulator (to improve turbulence and provide more effective heat transmission) and increasing the contact surface (through the installation of parts with unique geometry), which can be obtained from different turbulator used in other geometries. In this research, the limited volume method to solve governing equations in three-dimensional space and Cartesian coordinates has been used on the network using Ansys Fluent software. In order of comparison, turbulators SLT and then TRT is compared to other turbulators (TRT, SHT, RET) It has the highest Nusselt number, and in the Reynolds numbers in the turbulent flow regime, they have the most significant reduction in the friction coefficient.

* Corresponding author.
E-mail address: Pasha.pooya@yahoo.com (P. Pasha).

Peer review under responsibility of Faculty of Engineering, Alexandria University.

https://doi.org/10.1016/j.aej.2023.02.003

Nomenclature

ε	Attrition rate (No units)
f	Friction (N)
Re	Reynolds number
x, y	Coordinates (m)
u,v,w	Velocity components (m/s)
d	The square root of the cell (No units)
ϑ	Kinematic viscosity (m^2/s)
C_p	Specific heat at constant pressure (j/kg.k)
k	Thermal conductivity ($Wm^{-1}K^{-1}$)
P	Fluid pressure (pa)
f_0	Petukhov's correction factor
P_d	Dynamic pressure (pa)
T	Temperature (K)
T_w	Wall temperature ($k^{\cdot}$)
$g_y,\ g_x, g_z$	Gravitational acceleration (m/s^2)
Pr	Prandtl number (υ/α)
Nu	Nusselt parameter (dimensionlee)

Greek Symbols

ρ	Density (kg/m^3)
μ	Dynamic viscosity (kg/m. s)
τ	Shear stress (s^{-1})
σ	tension parameter

1. Introduction

In recent years, heat transfer improvement technology has been widely used in heat transfer applications such as industries refrigeration, automobile manufacturing, and oil, gas, and petrochemical process industries have been used. The purpose of employment of this technology is to achieve higher heat fluxes in heat transfer units. The outcomes of the utilization of this technology can be diminished to the converter level thermal impressions, reducing the difference in the driving temperature of the converters, which causes a decrease in entropy production and an increase in the efficiency of the second law thermodynamics, he pointed out. In fluid and thermal fields, MD. Shamshuddin and his colleagues [1–5] conducted studies on heat transfer and normal nanofluid flow, and Maxwell flow using FEM and FVM methods. In their studies, applications of changes in important physical and fluid parameters in the environment of porous channels and ship surfaces can be seen, which have been addressed using AnsysFluent software. A. Boonloi et al. [6] in 2020 regarding the improvement of thermohydraulic efficiency in the heat exchanger two equipped with a square duct containing an inclined square ring (*SI*) with an angle of 45 degrees published a review. This research is focused on the use of the passive method, and the sloped square ring, similar to a thin plate, in it has been used to improve the heat transfer rate and efficiency of the heat exchanger containing the square duct. The difference between values s/H and $b/$, changed the position of the eddy current penetration in the duct walls and also, the flow resistance Reduces or increases vortices. A. Verma et al. [7] in 2018, an article about increasing heat transfer and friction losses 4 in heat exchanger tubes containing modified spiral coils, published. This exposition is an approximately exploratory examination of heat exchange rate and liquid flow behavior in a tubular heat exchanger counting winding coils it has been modified. Zahra Azizi et al. [8] distributed a paper that heat exchangers are an imperative portion of heat units and are broadly utilized in mechanical units nowadays there are rural items change industries. Z. Xu et al. [9] An editorial in 2018 concerning the characteristics of heat exchange and distribute flow resistance in a channel with a quadrilateral area containing whirlpool current generators, which incorporates examination it is numerical and test and in it utilizing single-phase water working liquid on five sorts of turbines with regions the same side has been considered and concluded. When the semi-cylindrical eddy current generator is consecutively (perpendicular to the flow) placed next to the kennel wall, the thermohydraulic efficiency coefficient is the highest. Much attention has been paid in the field of the effects of using tubes in heat exchangers, especially regarding the turbulence phenomenon, Pressure drop, coefficient of thermal efficiency, dimensions of heat exchangers, and also types of turbulator. Turbulators, There are parts that, due to the creation of a rotating flow of fluid in the regime of smooth flow, it is directed towards and in the form of a turbulent flow and increases the heat transfer rate and, consequently the pressure drop and pumping power consumption [10–21]. The principal moot point in this investigation is heat removal from surfaces with high heat flux, which is the use of tabulators and parts with a particular geometry, it has been chosen as a solution to this moot point. The basic hypothesis in this investigation is to increase fluid heat transfer by increasing turbulence and heat transfer by increasing the plane of heat transfer and establishing a vortex flow. The purpose of employment of this technology is to achieve higher heat fluxes in heat transfer units. One of the technologies for improving heat transfer used in heat exchangers, which is called the most serious energy-consuming devices in process industries, is the part that increases internal thermal transfer it is a pipe or duct. The most obvious feature of using these devices is reducing heat transfer in heat exchangers. Among the other benefits of using these parts, it is possible to reduce the cost of initial construction and improve the performance of converters clogging deposits in the exchanger tubes, and improvement of flow distribution in the tubes of heat exchangers. Utilizing strategies to progress heat exchange, not as it cause a critical decrease in vitality utilization in handle industries3 it'll bring, but moreover, issues caused by the aggregation of silt in channels and conduits to a critical degree reduces. In this paper, turbulators SLT and then TRT is compared to other turbulators (TRT, SHT, RET) It has the highest Nusselt number and in the Reynolds numbers in the turbulent flow regime, they have the greatest reduction in the friction coefficient. Whereas the most pressure drop has occurred in these two types of turbulators. On the other hand, the efficiency of heat transfer in these two types of turbulator is more than other turbulators, and in terms of TKE values, it is in a more suitable position. The main problem in this research is heat removal from surfaces with high heat flux, and the use of turbulators and parts with special geometry has been chosen as a solution to this problem. The basic idea of this research is the simultaneous use of turbulators (To increase turbulence and provide more effective heat transfer) and increase the contact surface (through the installation of parts with special geometry), which can be used with different turbulators with different geometries. Investigating the changes of Nusselt number and displacement heat transfer coefficient with different Reynolds numbers and also investigating the profile-The temperature and the coefficient of thermal efficiency in the duct with a square section help to calculate the heat transfer rate. The innovation of this research is the simultaneous use of a turbulator (in order to increase turbulence and provide more effective heat transfer), and increasing the contact surface (through the installation of parts with special geometry) that can be obtained from different turbulators and used different geometries.

2. Problem definition and governing equations

To simulate the desired flow, at this stage, it is necessary to have a suitable model and geometry for simulating the flow chosen. Can be used to model the flow of the working fluid (single-phase water) in the duct (square section) equipped with different turbulators, the following simplification assumptions were used: The flow of the working fluid (single-phase water) is continuous: this assumption is based on the type of flow regime in molecular dimension determined. The investigated fluid is Newtonian and incompressible. In this research, the duct with a square cross-section without a turbulator and ducts with a cross-section a square equipped with turbulators with different geometries are compared with each other, so that in the duct without a turbulators, the slow flow regime is used, and in the duct equipped with a turbulators, the turbulent flow regime is used. Also, in the end, compare the behavior of the working fluid in the duct equipped with different turbulators. In this research, the temperature of the input fluid (single-phase water) is 300 degrees, and the heat flux is $100 \mathrm{w/m^2}$, and with properties Density $998.2\ \mathrm{kg/m^3}$, specific heat 4182 kg. K, thermal conductivity coefficient 6.0w/m and viscosity dynamic.0.001003 kg/m.s is considered. The length of the duct without turbulators is Lo = 200 mm and its sides are each a = 50 mm (smooth flow), according to Fig. 1a.The magnitude of the velocity of the working fluid is considered to be 0.5 s/m, so that the validation stage can be done in this way. The length of the duct containing the turbulator is Lc = 250 mm and its sides are each ac = 50 mm (turbulent flow). The types of turbulators investigated in this research, include turbulators SCT, SLT, SHT, RET, and TRT. Their dimensions are L_t = 200 *mm* length and at = 40 mm, with step P = 40 mm and thickness THK = 2 mm and angle of attack is. In this research, the limited volume method to solve governing equations in 3D space and Cartesian three-coordinates is used on the network.

To create a suitable and optimal geometry for the turbines and compare them with each other, five types of geometry are examined, which are placed in Fig. 1 respectively, the geometry of the semi-cylindrical turbulator (SCT), Semi-triangular turbulator (TRT), sharp point or sword (SHT), Semi-crescent turbulator (SLT), and rectangular turbulator (RET) is shown. The dimensions of all turbulators are LT = 200 mm, width is w_T = 40 mm and thickness is THKT = 0.2 mm. The geometry and dimensions of the vanes installed on the blades of the turbulator are shown in Fig. 1b. And the dimensions of the wings are length L_{wing} = 15 mm, width is W_{wing} = 15 mm with steps P_{wing} = 40 mm.

Table 1a, in duct without turbulator, using the Conforming Patch method, Tetrahedrons and Size Element type with 1.5 mm in medium mesh mode, and the size of 1.2 mm in fine mesh mode.

In the ducts containing the aforementioned turbulators, like the duct without turbulators, by the Conforming Patch method, Tetrahedrons and the type of Size Element are used, the information about each of them is in Tables 1b–1f and Fig. 1c have been shown.

2.1. Mathematical equations

As stated in the hypothesis area, the equations overseeing the material science of the issue are based on the k- ε pattern it includes continuity equations, movement size, and flow energy in the 3D Cartesian device for incompressible flow is communicated as takes after [9]:

$$\nabla.\rho\vec{V}+\frac{\partial\rho}{\partial t}=0 \tag{1}$$

$$\rho g_x+\frac{\partial\sigma_{xx}}{\partial x}+\frac{\partial\tau_{yx}}{\partial y}+\frac{\partial\tau_{zx}}{\partial z}-\rho\left(\frac{\partial u}{\partial t}+u\frac{\partial u}{\partial x}+v\frac{\partial u}{\partial y}+w\frac{\partial u}{\partial z}\right)=0 \tag{2}$$

$$\rho g_y+\frac{\partial\tau_{xy}}{\partial x}+\frac{\partial\sigma_{yy}}{\partial y}+\frac{\partial\tau_{zy}}{\partial z}-\rho\left(\frac{\partial v}{\partial t}+u\frac{\partial v}{\partial x}+v\frac{\partial v}{\partial y}+w\frac{\partial v}{\partial z}\right)=0 \tag{3}$$

$$\rho g_z+\frac{\partial\tau_{xz}}{\partial x}+\frac{\partial\tau_{yz}}{\partial y}+\frac{\partial\sigma_{zz}}{\partial z}-\rho\left(\frac{\partial w}{\partial t}+u\frac{\partial w}{\partial x}+v\frac{\partial w}{\partial y}+w\frac{\partial w}{\partial z}\right)=0 \tag{4}$$

$$\rho\left(\frac{\partial u}{\partial t}+u\frac{\partial u}{\partial x}+v\frac{\partial u}{\partial y}+w\frac{\partial u}{\partial z}\right)-\rho g_x+\frac{-\partial P}{\partial x}-\mu\left(\frac{\partial^2 u}{\partial x^2}+\frac{\partial^2 u}{\partial y^2}+\frac{\partial^2 u}{\partial z^2}\right)=0 \tag{5}$$

$$\rho\left(\frac{\partial v}{\partial t}+u\frac{\partial v}{\partial x}+v\frac{\partial v}{\partial y}+w\frac{\partial v}{\partial z}\right)-\rho g_y+\frac{-\partial P}{\partial y}-\mu\left(\frac{\partial^2 v}{\partial x^2}+\frac{\partial^2 v}{\partial y^2}+\frac{\partial^2 v}{\partial z^2}\right)=0 \tag{6}$$

$$\rho\left(\frac{\partial w}{\partial t}+u\frac{\partial w}{\partial x}+v\frac{\partial w}{\partial y}+w\frac{\partial w}{\partial z}\right)-\rho g_z+\frac{-\partial P}{\partial z}-\mu\left(\frac{\partial^2 w}{\partial x^2}+\frac{\partial^2 w}{\partial y^2}+\frac{\partial^2 w}{\partial z^2}\right)=0 \tag{7}$$

$$\frac{\partial(\rho c_p uT)}{\partial x}+\frac{\partial(\rho c_p vT)}{\partial y}+\frac{\partial(\rho c_p wT)}{\partial z}-\frac{\partial}{\partial x}\left(k\frac{\partial T}{\partial x}\right)-\frac{\partial}{\partial y}\left(k\frac{\partial T}{\partial y}\right)-\frac{\partial}{\partial z}\left(k\frac{\partial T}{\partial z}\right)=0 \tag{8}$$

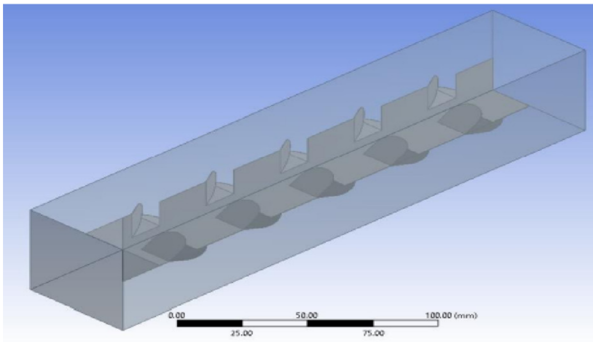

a) The geometry of the duct equipped with the SLT turbulato.

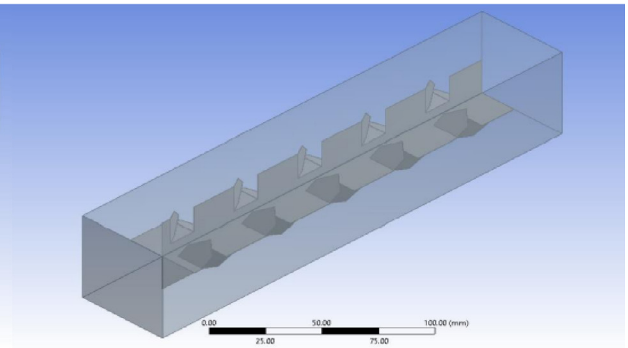

b) The geometry of the duct equipped with the TRT turbulator.

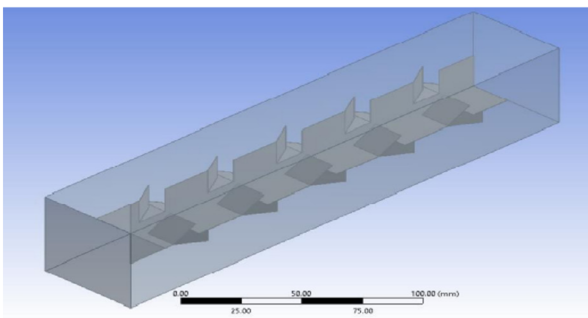

c) The geometry of the duct equipped with the RET turbulator.

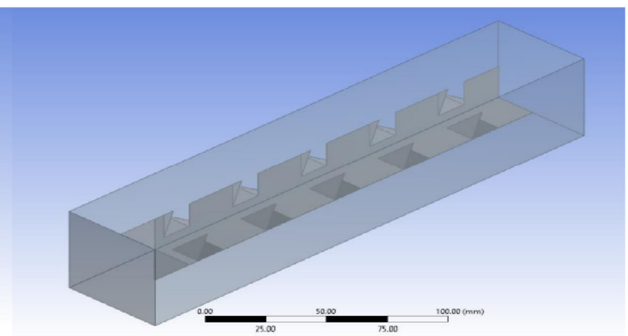

d) The geometry of the duct equipped with the SHT turbulator.

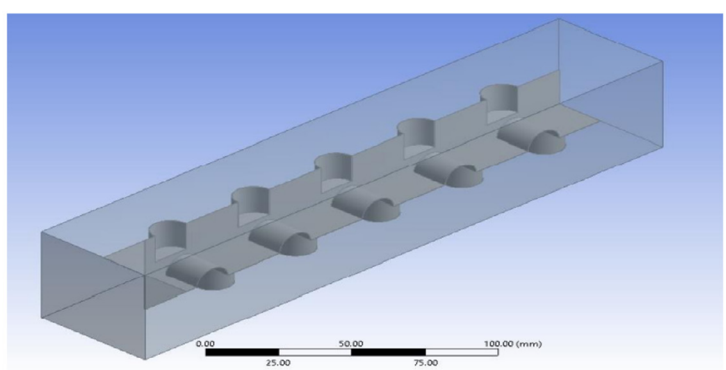

e) The geometry of the duct equipped with the SCT turbulator.

Fig. 1a The geometry of the duct equipped with the different types of turbulators.

Equation (1) is related to continuity, Equations (2)–(4) are related to the equations of motion, and Equations (5)–(8) are related to the Navier stocks equations and energy. It should be noted that in the above equations, ρ is the density, (u, v, w) are the velocity in the three directions, g is the acceleration, P is the fluid pressure, μ is the dynamic viscosity,τ is the shear stress,σ is the tension parameter C_p is the Specific heat, k is the Thermal conductivity, T is the temperature and t is the time function. Shear stress may be a component of push on the surface of a protest. Shear stretch is from the constrain vector opposite to the typical vector of the cross-section. Dynamic viscosity evaluates the inner frictional constraint between adjoining layers of liquid that are in relative motion. According to the geometry of the duct (square cross-section) and the above-mentioned turbines (5 types), the boundary conditions used in the Ansys Fluent software are discussed in detail below this paragraph. **Inlet boundary conditions:** In the input area, the velocity of the component, quantified, and velocity magnitude in this article in the duct without turbulator and the duct with the turbulator is considered to be 0.5 s/m (same as the refer-

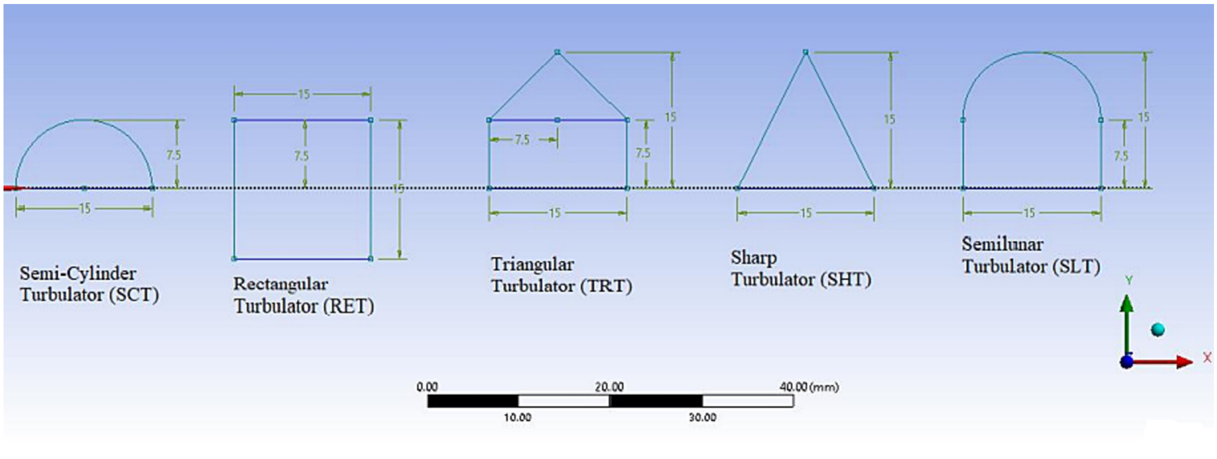

Fig. 1b The geometry and dimensions of the flaps installed on the blades of the turbulator.

Table 1a Specifications of the network related to the duct without turbulator.

Mesh Specifications for Duct without Turbulator	
Method:	Patch Conforming, Tetrahedrons
Body Size Type:	Element Size
Size Function:	Curvature
Quality:	Medium
Medium Mesh:	Element Size: 1.5 mm
	Nodes: 1,758,853
Fine Mesh:	Elements: 1,284,587
	Nodes: 3,410,477

Table 1b Specifications of the network related to the duct with turbulator by SLT model.

Mesh Specifications for Duct without Turbulator	
Method:	Patch Conforming, Tetrahedrons
Body Size Type:	Element Size
Size Function:	Curvature
Quality:	Medium
Medium Mesh:	Elements: 15,715,415
	Nodes: 2,692,943

Table 1c Specifications of the network related to the duct with turbulator by TRT model.

Mesh Specifications for Duct without Turbulator	
Method:	Patch Conforming, Tetrahedrons
Body Size Type:	Element Size
Size Function:	Curvature
Quality:	Medium
Medium Mesh:	Elements: 10,517,421
	Nodes: 1,805,796

ence article). Inlet pressure as a reference pressure and equal to zero the temperature of the input fluid and the heat flux are 300 and 100 w / m^2 respectively. **Outlet boundary conditions:**

Table 1d Specifications of the network related to the duct with turbulator by SHT model.

Mesh Specifications for Duct without Turbulator	
Method:	Patch Conforming, Tetrahedrons
Body Size Type:	Element Size
Size Function:	Curvature
Quality:	Medium
Medium Mesh:	Elements: 15,711,910
	Nodes: 2,691,558

Table 1e Specifications of the network related to the duct with turbulator by RET model.

Mesh Specifications for Duct without Turbulator	
Method:	Patch Conforming, Tetrahedrons
Body Size Type:	Element Size
Size Function:	Curvature
Quality:	Medium
Medium Mesh:	Elements: 10,542,910
	Nodes: 1,808,558

Table 1f Specifications of the network related to the duct with turbulator by SCT model.

Mesh Specifications for Duct without Turbulator	
Method:	Patch Conforming, Tetrahedrons
Body Size Type:	Element Size
Size Function:	Curvature
Quality:	Medium
Medium Mesh:	Elements: 10,531,910
	Nodes: 1,811,558

In this type of border, due to the uncertainty of the development of the working fluid inside the duct, changes in the directions of the coordinate axes are considered opposite to zero and if the changes in one of the directions of the axes consider zero coordinates, applying this boundary condition will cause

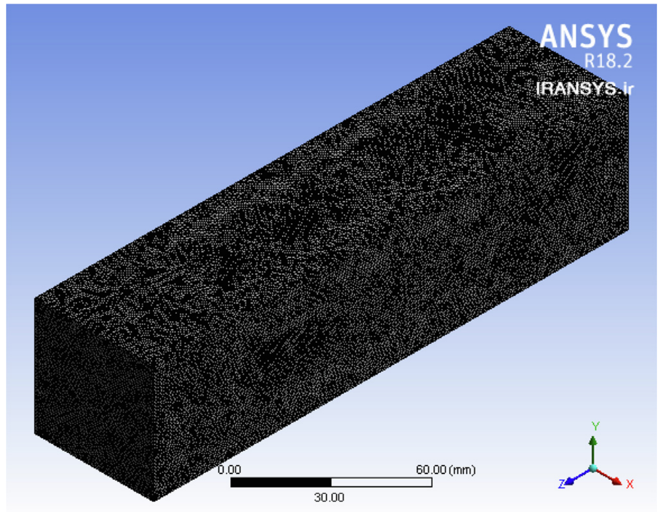

Fig. 1c Geometry of the mesh.

errors in the flow equations. **Wall boundary conditions:** One of the most critical and practical boundary conditions is the wall boundary condition, its selection is thus considered it is assumed that the wall does not move or in other words is still and fixed and the velocity gradient on it is zero or condition of non-slip established The thermal boundary condition can be one of three Dirichlet conditions Newman or displacement. Constant temperature, constant heat flux, and displacement the boundary are the three boundary conditions used in the numerical code this is the research that is described in the following related relationships:

Boundary condition of constant temperature (Dirichlet) is as follows [9]:

$$TBoundary = TWall = Constant \tag{9}$$

Constant flux boundary condition (Newman) [9]:

$$TBoundary = Ti + \frac{q_{Boundary}}{(ki/\delta xi)} \tag{10}$$

Displacement boundary condition [9]:

$$TBoundary = \frac{(ki/\delta xi)Ti + hT\infty}{(ki/\delta xi/) + h} \tag{11}$$

In the above relations, the index (i) is associated with the first point adjacent to the boundary, and the index is related to the environment. Solving linearized algebraic equations should be done by iterative methods such as the Galerkin method, Method of least squares, method of sharing, and Riley-Ritz method and be used like this. Methods and ways of iteration are started based on the initial guess and are repeated until the total error is less than an acceptable limit. The most common method used in this research, which is done by software, is the method of least squares. To get the velocity area, the momentum equation must be solved first, but the field needed to solve it is pressure. Because pressure is an important part of the equation of motion and so far relation it is not provided to determine the pressure area. In this research, to solve the equations governing the physics of the problem, from Simple algorithm is used on the network.

2.1.1. Finite volume method

The Finite Volume Method (FVM) may be a strategy for representing and assessing halfway differential equations within the frame of arithmetical conditions. Within the limited volume strategy, volume integrands in a halfway differential condition that contain a dissimilarity term are changed over. The Finite Volume Method (FVM) could be a discretization strategy for the estimation of a single or a framework of fractional differential conditions communicating the preservation, or adjustment, of one or more quantities. The FVM may be a regular choice for solving CFD issues since the PDEs you have got to resolve for CFD are preservation laws. Be that as it may, you'll be able also use both FDM and FEM for CFD, as well. The FVM's most significant advantage is that it should do flux assessment for the cell boundaries.

2.2. Parameters and assumed values in the numerical solution method

In a duct without a turbulator, the relaxation coefficient or the return to rest factor Parameters such as Pressure, density, volume forces, movement size (momentum), and energy are entered into the software with the following values are:

$$\begin{aligned}\mathbf{P} &= 0.3,\ \mathbf{D}\text{ensity} = 1,\ \mathbf{B}\text{ody Forces} = 1,\ \mathbf{M}\text{omentum}\\ &= 0.6,\ \mathbf{E}\text{nergy} = 0.8\end{aligned} \tag{12}$$

For ducts equipped with turbulators, relaxation coefficient of pressure parameters, density, volume forces, Movement size (momentum), turbulent flow kinetic energy, turbulent flow spreading rate, and flow viscosity disturbed with the following values are entered in the software:

$$\begin{aligned}\mathbf{P} &= 0.3,\ \mathbf{D}\text{ensity} = 1,\ \mathbf{B}\text{ody Forces} = 1,\ \mathbf{M}\text{omentum}\\ &= 0.6,\ \mathbf{E}\text{nergy} = 0.8,\ \mathbf{T}\text{urbulence Kinetic Energy}\\ &= 0.8,\ \mathbf{T}\text{urbulence }\mathbf{D}\text{issipation Rate}\\ &= 0.8,\ \mathbf{T}\text{urbulence Viscosity} = 1\end{aligned} \tag{13}$$

2.3. Independence from the network

The results of a simulation are reliable and reliable when the results are independent of the mesh or network and do not change by changing the number of nodes and elements. For this purpose, two types of mesh, medium mesh, and fine mesh are used for the duct without a turbulator (Fig. 1c). The results of a simulation are reliable when the results are independent of the mesh or network, by changing the number of nodes and elements, does not change them. For this purpose, a duct without a turbulator of two types of mesh, medium and very small, has been used, which has 853,758,1 nodes, 587,284,1elements, and 477,410,3 nodes, 960,504,2 elements, and the results obtained for both ducts (with mesh) medium and excellent mesh (in the graphs related to dynamic pressure and axial velocity in the center of the duct and along the z-axis, the forms (2-a) to (2-d) are shown and can be compared. According to the comparison, it has been concluded that with the finer grid of the meshes and the increase in the number of elements, there are changes in the parameters of the fluid velocity and dynamic pressure, which has resulted in an increase in the velocity gradient.

As can be seen in both types of mesh (Fig. 2), the graphs related to dynamic pressure and axial velocity it has almost the same results, and all the governing equations and considered parameters have it will bring relevant and reliable results.

3. Validation

To ensure the correctness of the numerical results extracted with the help of the software and its compatibility with the research results of Zhiming and his colleagues, for a duct with

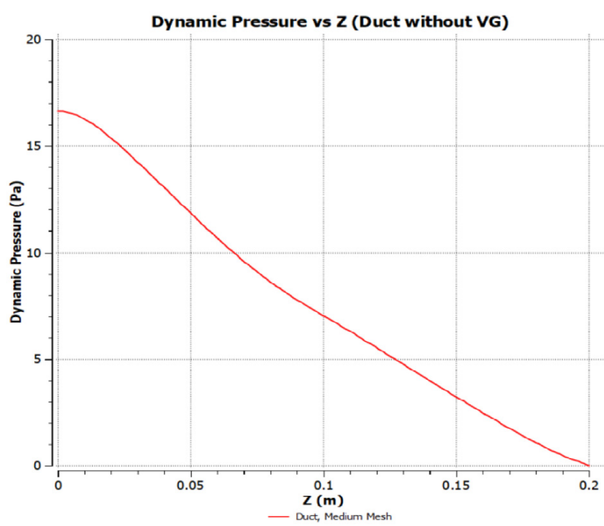

a) Dynamic pressure changes of the fluid according to the duct length without a turbulator with an average mesh.

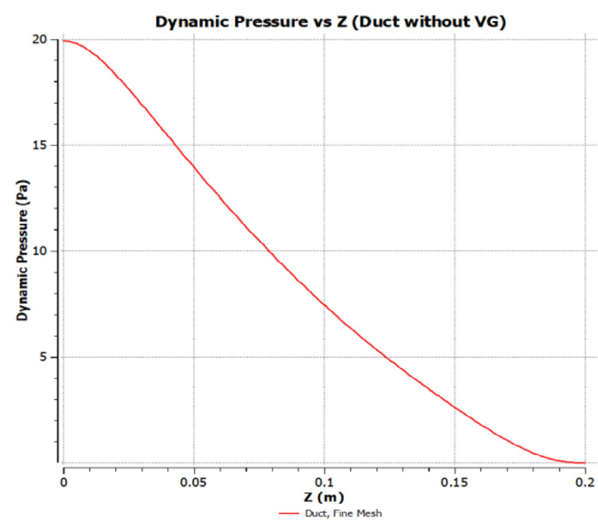

b) Dynamic pressure changes of the fluid according to the duct length without a turbulator with a small mesh.

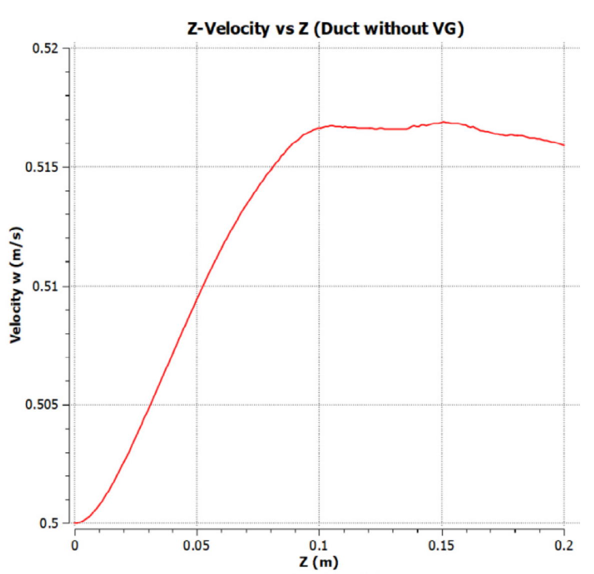

c) Variations of fluid axial velocity according to the duct length without a turbulator with medium mesh.

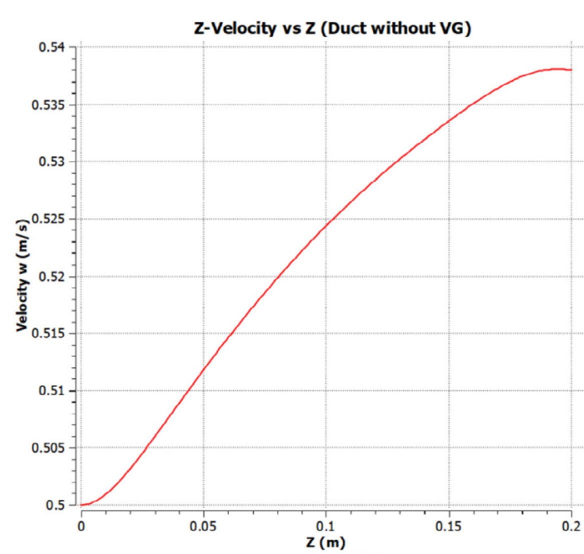

d) Variations of fluid axial velocity according to the duct length without a turbulator with small mesh.

Fig. 2 Variations and dynamic pressure of fluid according to the length of the duct without a turbine with a small and medium mesh.

a square cross-section without a turbocharger and containing a semi-cylindrical turbocharger by Taking the boundary conditions and applied formulas in the Reynolds number range from 10,000 to 30,000, the following steps have been performed. Now the Reynolds number is defined. In fluid mechanics, the Reynolds number (Re) may be a dimensionless quantity that makes a difference in foreseeing liquid stream designs in several circumstances by measuring the proportion between inertial and thick strengths.

Formulas used:

Nilinski's formula [9]:

$$Nu_0 = \frac{\left(\frac{\varepsilon}{8}\right)(Re - 1000)Pr}{1 + 12.7(\varepsilon/8)^{\frac{1}{2}}(pr^{2/3} - 1)} \tag{14}$$

(3 * 103 < Re < 5 * 106, $0.5 \leq Pr \leq 2000$).

Pr is the Prandtl number, Filonenko formula [9]:

$$\varepsilon = (1.82.\log Re - 1.64)^{-2} \tag{15}$$

(104 < Re < 106).

In this formula, N_{u0} represents the Nusselt number for the duct without a turbocharger and the Prandtl number for fluid with an inlet temperature of 300 degrees Kelvin; and ε attrition rate, it is obtained from the following equation [9]:

Table 2 The parameters related to the duct without turbulator and the duct with in turbulator terms of Reynolds number.

Re_0	Nu_0	f_0	$\Delta p(Pa.)$	f	Nu	j/j_0	f/f_0	R*-Nu/Nu_0
10,000	74.540432	0.03148	127.365	0.05823	53.097	1.4714	1.85	0.71233
12,000	88.035618	0.02993	121.097	0.05537	61.693	1.4442	1.85	0.70077
14,000	101.12612	0.02870	116.151	0.05311	70.038	1.4263	1.85	0.69258
16,000	113.89035	0.02770	112.108	0.05121	78.174	1.4125	1.85	0.68640
18,000	126.38277	0.02687	108.714	0.04970	86.131	1.4018	1.85	0.68151

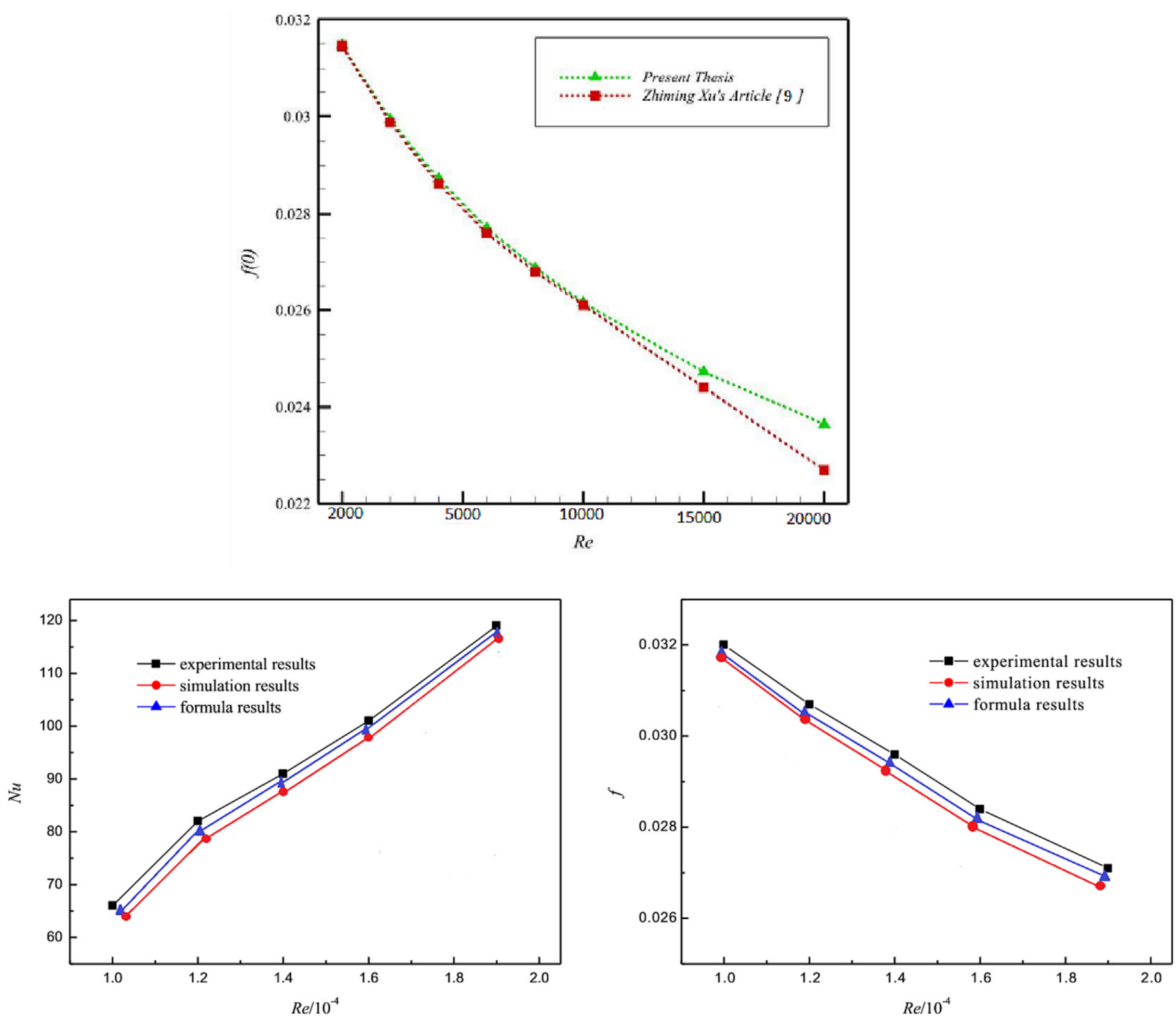

Fig. 3 Comparison of friction parameters and Nusselt number of the present work with Dr. Zhiming's article [9] and other laboratory results in the duct without turbulator.

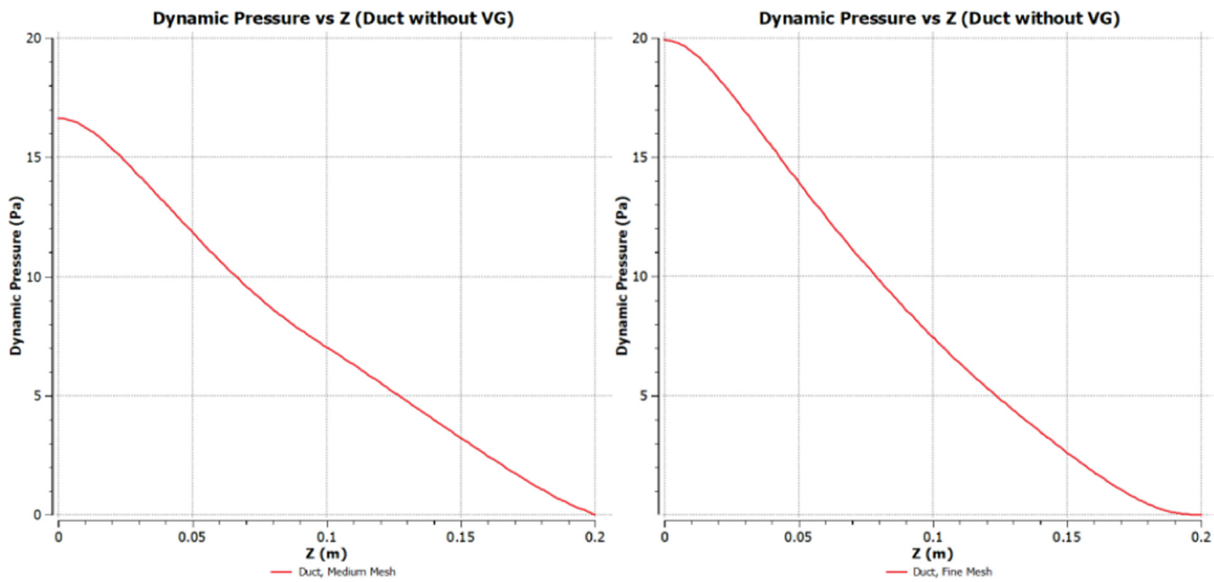

Fig. 4 Fluid dynamic pressure in terms of the duct length without turbulator with medium mesh and fine mesh.

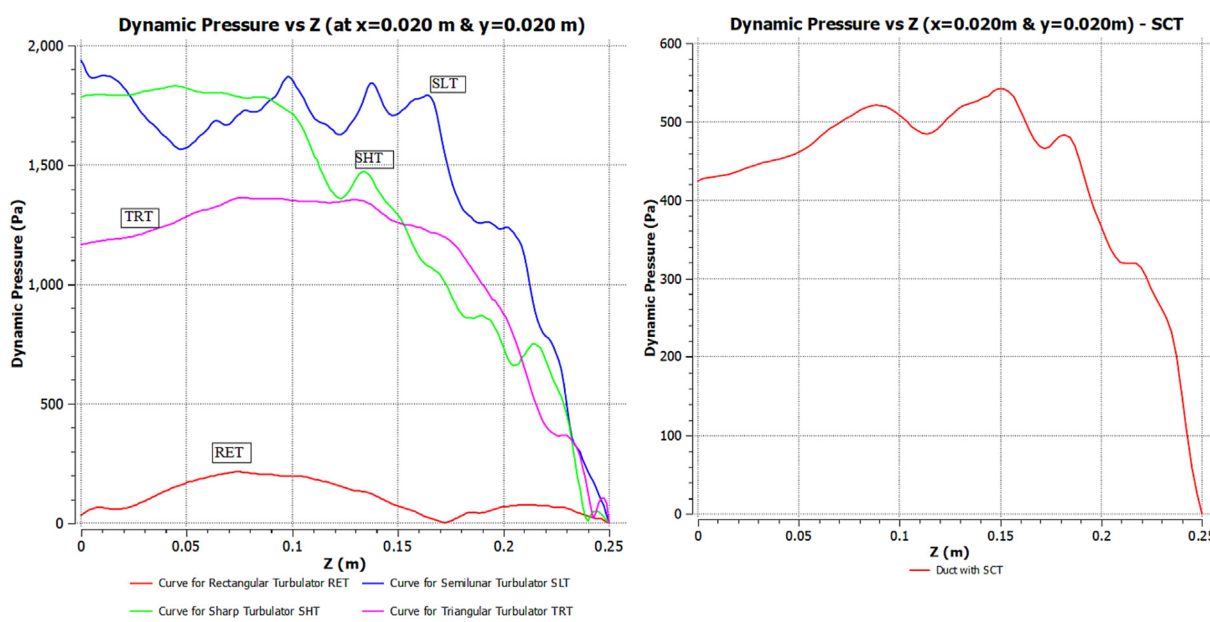

Fig. 4a Fluid dynamic pressure according to the duct length equipped with SCT, SLT, TRT, RET, and SHT turbulators in the coordinates x = 20 mm and y = 20 mm.

$$pr_{300^k} = \frac{\mu c_p}{k} = \frac{(0.8509)(4.18133)}{0.6} = \frac{5}{93} \quad (16)$$

And also Petukhov's correction factor:

$$f_0 = (0.79 LnRe - 1.64)^{-2} \quad (17)$$

To calculate the coefficient of friction in a duct equipped with a turbulator, the following equation is used:

$$f = \frac{2\Delta p.A_c}{\rho A_0 u^2} \quad (18)$$

Its average value will be 1.85 for all turbulators, and f is the friction parameter.

By obtaining the value of (f), the values related to R_{e0} can be calculated and obtained from the following formula:

$$Re_0 = [\frac{Re^3 c.f}{0.07}]^{0.363} \quad (19)$$

According to the specified values of Re and the Prandtl number obtained above, the Nusselt number related to the duct can be obtained equipped with a semi-cylindrical turbulator was determined from the following relationship:

$$Nu = 0.0133 Re^{0.823} (Pr)^{0.4} \quad (20)$$

Table 3 Investigating dynamic pressure changes along the channel with various meshes and turbulators.

Dynamic Pressure (Pa)												
Duct Length	Z = 10 mm	Z = 15 mm	Z = 20 mm	Z = 35 mm	Z = 60 mm	Z = 90 mm	Z = 125 mm	Z = 170 mm	Z = 190 mm	Z = 200 mm	Z = 220 mm	Z = 230 mm
Duct, Medium Mesh	16.26263	15.85744	15.35416	13.62576	10.63773	7.818501	5.174996	1.764159	0.484935	1.1E−05	N.A.	N.A.
Duct, Fine Mesh	19.44765	18.94275	18.31951	16.16006	12.47303	8.547871	4.893692	1.072966	0.095534	6.66E−07	N.A.	N.A.
SCT	N.A.	432.8301	N.A.	449.4919	480.3997	521.1549	505.1007	467.9644	447.4739	367.3701	313.3824	261.248
TRT	N.A.	1188.431	N.A.	1229.884	1315.443	1358.904	1350.575	1208.065	1002.381	879.4741	407.3926	366.6754
RET	N.A.	58.1114	N.A.	114.078	193.0036	202.6945	147.6858	6.559896	42.61833	67.44406	72.46558	62.00677
SHT	N.A.	1792.498	N.A.	1817.725	1802.888	1770.054	1364.658	1044.844	868.8752	741.8619	686.6046	452.0233
SLT	N.A.	1866.146	N.A.	1660.258	1655.448	1770.209	1647.718	1660.612	1257.672	1239.996	785.049	494.6617

Colburn Factor is a dimensionless number that is a suitable analogy for heat transfer, movement size, and mass. Number Colburn relates the friction coefficient to the heat transfer coefficient. In turbulent flow, it is always possible, to use this number, but in slow flow, if the pressure gradient is high, the accuracy of the following relation is doubted.

$$j = \frac{Nu}{Re.Pr^{\frac{1}{3}}} \tag{21}$$

Nu is the Nusselt number, the ratio j/j is calculated from the following equation:

$$\frac{j}{j_0} = \frac{Nu}{Nu_0}\frac{Re_0}{Re} = \frac{0.0133Re^{0.823}(Pr)^{0.4}}{Nu_0}\frac{Re_0}{Re} \tag{22}$$

Factor related to system performance evaluation criteria (PEC) which includes a duct without a turbulator and a duct equipped with the following formula is used:

$$R.(PEC) = \frac{Nu}{Nu_0} \tag{23}$$

To obtain and calculate the difference in the inlet and outlet fluid pressure in the duct containing the semi- turbulator cylindrical, formula (24) can be used:

$$f = \frac{2\Delta P.A_c}{\rho A_0 u^2} \tag{24}$$

With the explanations and presentation of the mentioned formulas, the obtained results are related to the numerical validation of the current thesis Zhiming Zhu's article is according to the Table 2, and Fig. 3 is displayed accordingly. According to Fig. 3, a comparison has been made between the results of changes in the Nusselt number and the friction parameter of the present work with the numerical results and the experimental results of Dr. Zhiming and his colleagues [9]. According to the results of the solutions, the convergence between the changes of the Nusselt number and the friction coefficient in both articles has been done well and the numerical error has reached its minimum value.

4. Results and discussion

According to the fluid dynamic pressure formula (mentioned in the previous chapter) and checking this parameter along the axis of the duct in coordinates x = 20 mm and y = 20 mm for 5 types of turbulator and comparing them with each other and with duct without it has been obtained (3a) to (3b) shapes, Medium & Fine Mesh.

As can be seen (Fig. 4 and Fig. 4a), the maximum dynamic pressure of the working fluid in the ducts without turbulators with mesh medium and fine mesh, in Z = 10 mm, and the lowest occurred in Z = 200 mm. And also in the ducts containing turbulator, we have: In SLT and TRT, the most increased dynamic pressure is at Z = 150 and Z = 75 mm, respectively, and its lowest at z = 230 mm, in RET, the highest dynamic pressure is at Z = 75 mm and the lowest at z = 170 mm, Also, the most increased and lowest values of dynamic fluid pressure, comparatively, among the turbocharger-equipped ducts, respectively, are related to:

$$P_{Dyn.max} = 202.15paatZ = 90mm, P_{Dyn.min} = 42.62paatZ = 190mm \rightarrow RET$$

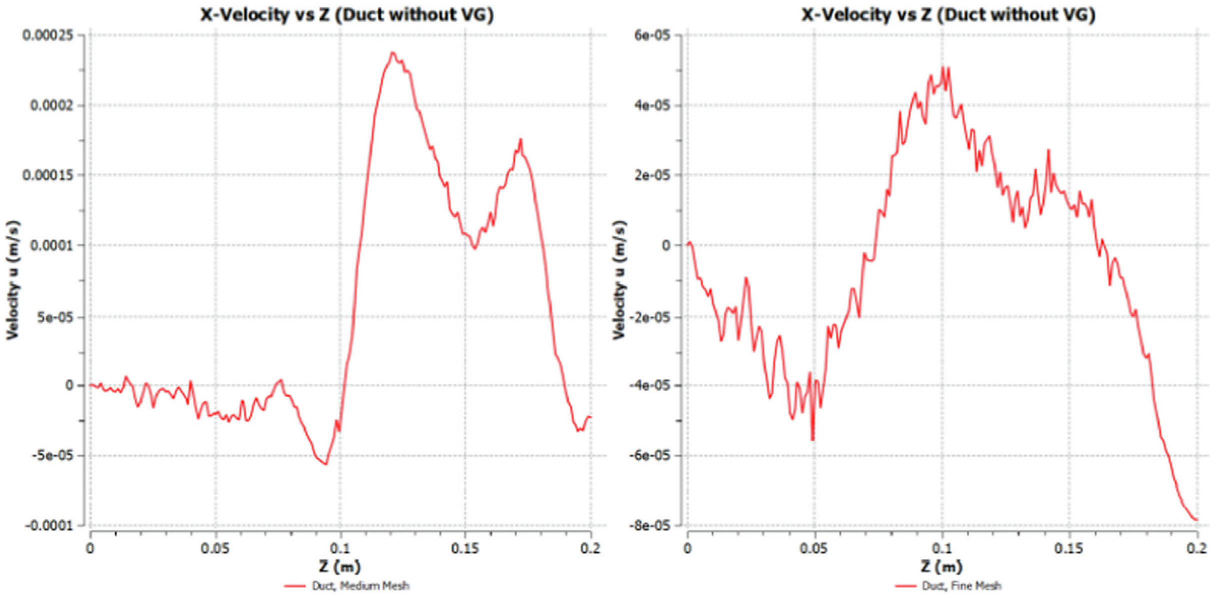

Fig. 5 Variations of the × - component of the fluid velocity according to the duct length without a turbulator with medium mesh and fine mesh.

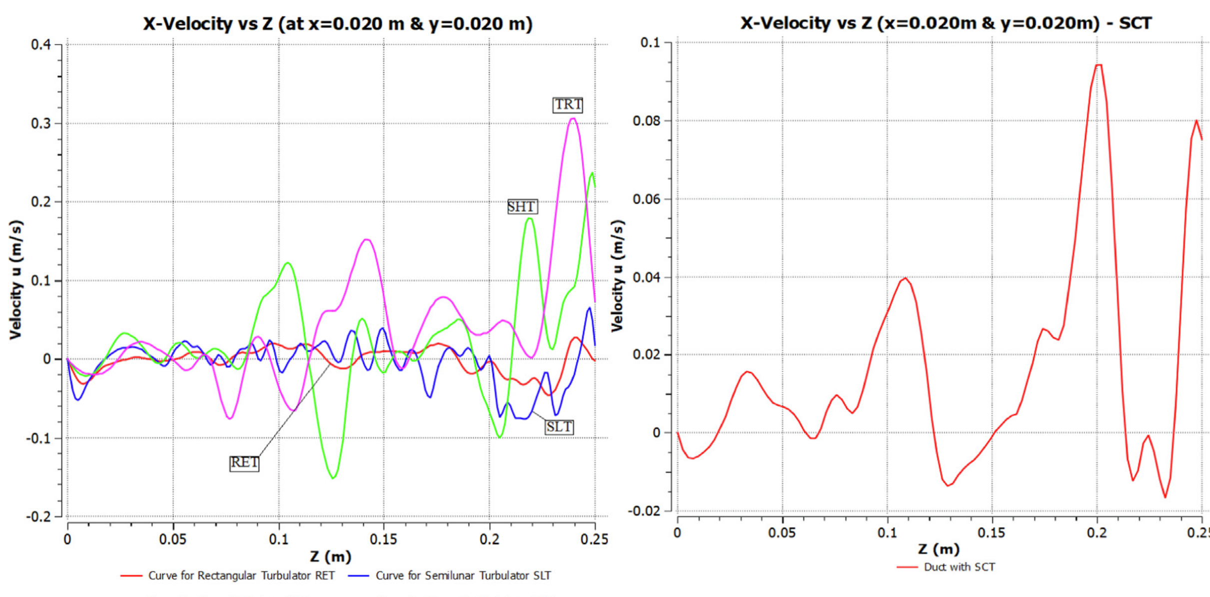

Fig. 5a Variations of the x- component of the fluid velocity according to the duct length equipped with turbulators SCT, SHT, SLT, RET and TRT.

In all the ducts (with and without turbulator) the trend of dynamic fluid pressure is almost descending and different levels of dynamic pressure have occurred (see Table 3).

As can be seen, the highest dynamic pressure of the working fluid in ducts without turbulator (Medium & Fine Mesh) occurred at Z = 10 mm and the lowest at Z = 200 mm. Also, the highest and lowest values of the dynamic pressure of the working fluid, comparatively, among the ducts equipped with turbulator, respectively, are related to SLT ($P_{Dyn.max.}$) = 1866.15 at Z = 15 mm, $P_{Dyn.min.}$) = 494.66 at Z = 230 mm) and RET ($P_{Dyn.max.}$) = 202.70 at Z = 90 mm, $P_{Dyn.min..}$) = 42.62 at Z = 190 mm). In all ducts (with turbulator and without turbulator), the trend of fluid dynamic pressure is almost descending, but at different pressure levels.

The x-component of the velocity in the duct without a turbulator is very small, which is quite apparent (Figs. 5–6a) . It should be noted that due to this subject, these parameters are not considered in future investigations and more on the subject of ducts containing turbulator are treated with different geometries. As can be seen in the ducts containing the tur-

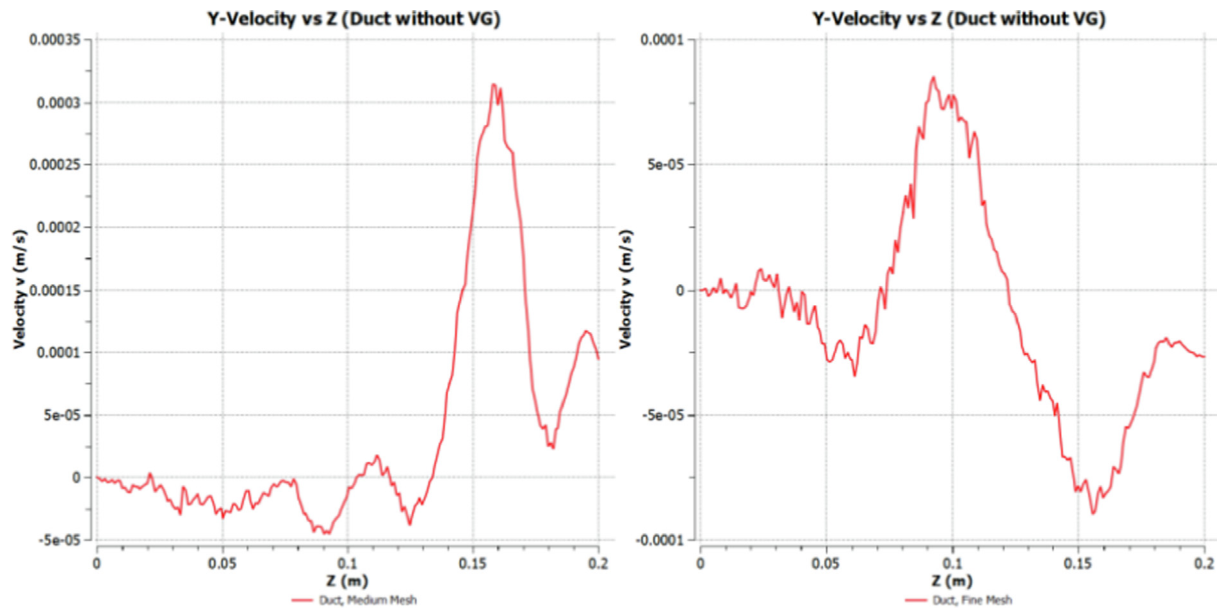

Fig. 6 Variations of the y- component of the fluid velocity according to the duct length without a turbulator with medium mesh and fine mesh.

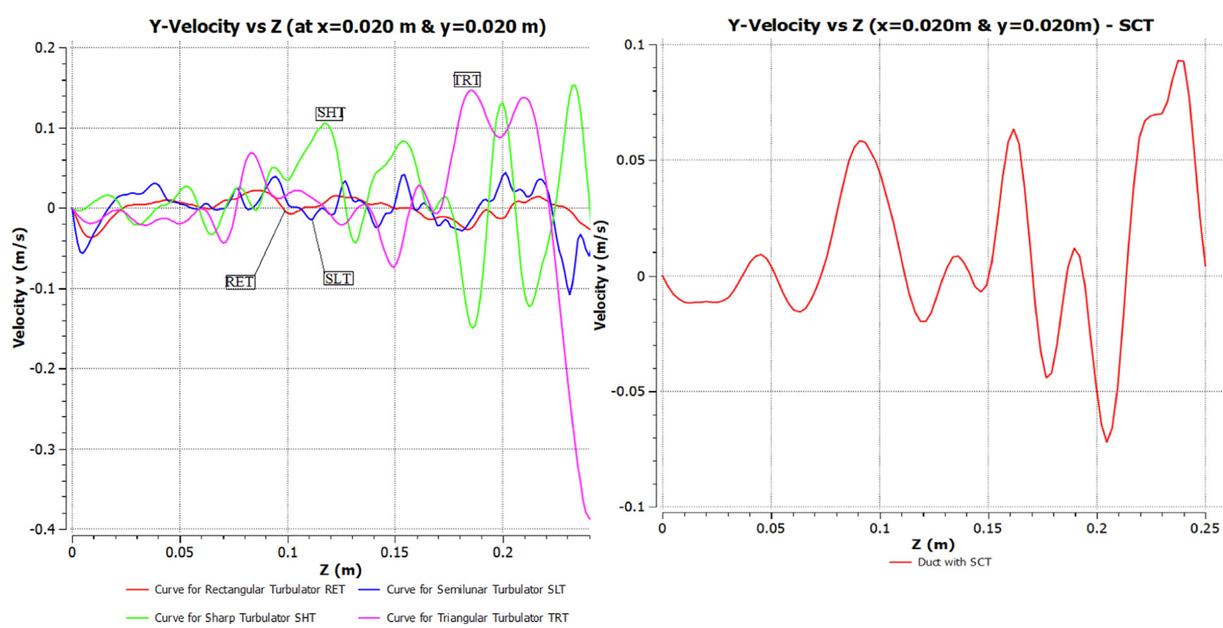

Fig. 6a Variations of the y- component of the fluid velocity according to the duct length equipped with turbulators SCT,SHT, SLT, RET and TRT.

bocharger, the maximum values of the × fluid velocity component (in the range turbulator) happened after Z = 200 mm, and the highest × component of the maximum velocity, corresponding to the SHT turbulator u = 0.18 m.s and the lowest × component of the maximum velocity corresponds to RET (u = 0.04 m.s).

The y - component of the fluid velocity along the z - axis in the mentioned coordinates for the ducts containing 4 types of turbulators, so from Z = 190 mm, it happened that the highest component of the maximum velocity corresponds to TRT (v = 0.21 m.s) and the lowest component the maximum velocity corresponds to RET (v = 0.21 m.s). The summary of the investigation of the y component of fluid velocity in ducts without turbulator and containing it is given in the table below (see Table 4):

About the axial velocity (z component of the working fluid velocity) in the 5 proposed turbulator types (according to Fig. 7), the following graphs in the coordinates x = 20 mm, and y = 20 mm have been studied and compared with each other. The important point is the presence of gravitational

Table 4 Investigating fluid velocity changes along the y direction along the channel with various meshes and turbulators.

Y-Velocity (m/s)												
Duct Length	Z = 10 mm	Z = 15 mm	Z = 20 mm	Z = 35 mm	Z = 60 mm	Z = 90 mm	Z = 125 mm	Z = 170 mm	Z = 190 mm	Z = 200 mm	Z = 220 mm	Z = 230 mm
Duct, Medium Mesh	−8.97E−06	−7.17E−06	−4.84E−06	−9.91E−06	−1.1E−05	−3.96E−05	−3.83E−05	0.0001774	8.8E−05	9.438E−05	N.A.	N.A.
Duct, Fine Mesh	1.235E−07	−6.93E−06	−8.14E−07	1.367E−06	−2.79E−05	7.437E−05	−9.38E−06	−5.54E−05	−2.03E−05	−2.66E−05	N.A.	N.A.
SCT	N.A.	−0.011602	N.A.	−0.002634	−0.01471	0.0580832	−0.014549	0.0096915	0.012022	−0.048918	0.0604846	0.0703346
TRT	N.A.	−0.010138	N.A.	−0.021033	−0.001043	0.0376223	−0.020718	−0.006694	0.1319689	0.0895129	0.0340498	−0.208531
RET	N.A.	−0.023036	N.A.	0.0052498	0.0004439	0.0209888	0.0146886	−0.012255	−0.008588	−0.013029	0.0100634	−0.000969
SHT	N.A.	0.0154728	N.A.	−0.011716	−0.012825	0.0336397	0.0467281	0.0029811	−0.109191	0.1308432	−0.055593	0.1190915
SLT	N.A.	−0.007618	N.A.	0.0255222	0.0025786	0.0263425	0.0179483	−0.021387	0.0057573	0.0404126	0.0285825	−0.097176

force and acceleration of gravity g = -9.81 m/s2, which has caused differences in the graphs and results obtained. As can be seen from the above graphs and the final tables extracted below for these 5 types of turbulators, there are still 5 jumps or jumps, as there are different plates in the shape of the blades, and apart from the RET type, 4 other types have this characteristic. are. The highest z component of the fluid velocity from the maximum point of view is related to SHT and TRT types and the lowest one is related to the SLT type. According to the values obtained from Table 5, the biggest axial speed difference is related to TRT, SCT and SHT types respectively, and the output speed value has increased compared to the input speed, and in SLT and RET types, this speed difference has been negative. And this means that the exit velocity of the fluid has decreased compared to the entry velocity.

The kinematic energy of the turbulent flow (Fig. 8), which is equal to the average kinetic energy of the working fluid per unit mass, has been investigated in 5 types of turbulators at the coordinates x = 20 mm, y = 20 mm and x = 20 mm, y = 20 mm and along the z axis. The corresponding graphs are shown below. As can be seen in both coordinates, the turbulent flow kinematic energy (TKE) in the semi-cylindrical turbulator (SCT) was almost similar and had a current difference, and also in the SLT and RET turbulators, it was almost without ups and downs, and within a certain range. They fluctuated a little, but SHT and TRT turbulators, had the most fluctuation and had the maximum value. The summary of the obtained values related to the TKE parameter is shown in the table below (Table 6).

According to all the tables and figures related to the ducts equipped with 5 turbulator and the resulting results, Aggregate and comparable forms of Nusselt number, friction coefficient, the ratio of Colburn coefficients, and pressure drop, in terms of numbers the Reynolds number in the turbulent flow range from 3000 to 12,000 is shown below, Figs. 9–12.

In heat transfer, the Nusselt number indicates the rate of displacement heat transfer to conductive heat transfer. A number a Nusselt greater than unity indicates a higher displacement heat transfer, and the larger this number is, the transfer more heat transfer is done. However, referring to Fig. 9, The highest value of Nusselt number obtained in 5 turbulators is related to SLT with Nu = 693.93 %, TRT with Nu = 565.23 %, SCT with Nu = 144.47 %.

Another important quantity was to obtain the coefficient of friction inside the duct. According to the formula Petukhov, the coefficient of friction inside the duct can be calculated according to different values of Reynolds number in Fig. 10. As it can be seen from diagram 2, with the increase of the Reynolds number, the value of the friction coefficient decreased, and the largest decrease is related to SLT (52.22 %) in the Reynolds number range 2500–31000, TRT (43.33 %) in Reynolds number ranged 9000–90,000, SCT (22.22 %) in Reynolds number ranged 27,000–80000, SHT (17.78 %) in Reynolds number ranged 28,000–650,000 and RET (8.33 %) in Reynolds number ranged 20,000–30000.

Another parameter that has been studied and compared is the ratio of Colburn coefficients (coefficient without the dimension of heat transfer) If this ratio is greater than unity, it shows that the heat transfer efficiency is the duct equipped with a turbulator has performed better than the duct without a turbulator. According to Fig. 11 and the calculated values

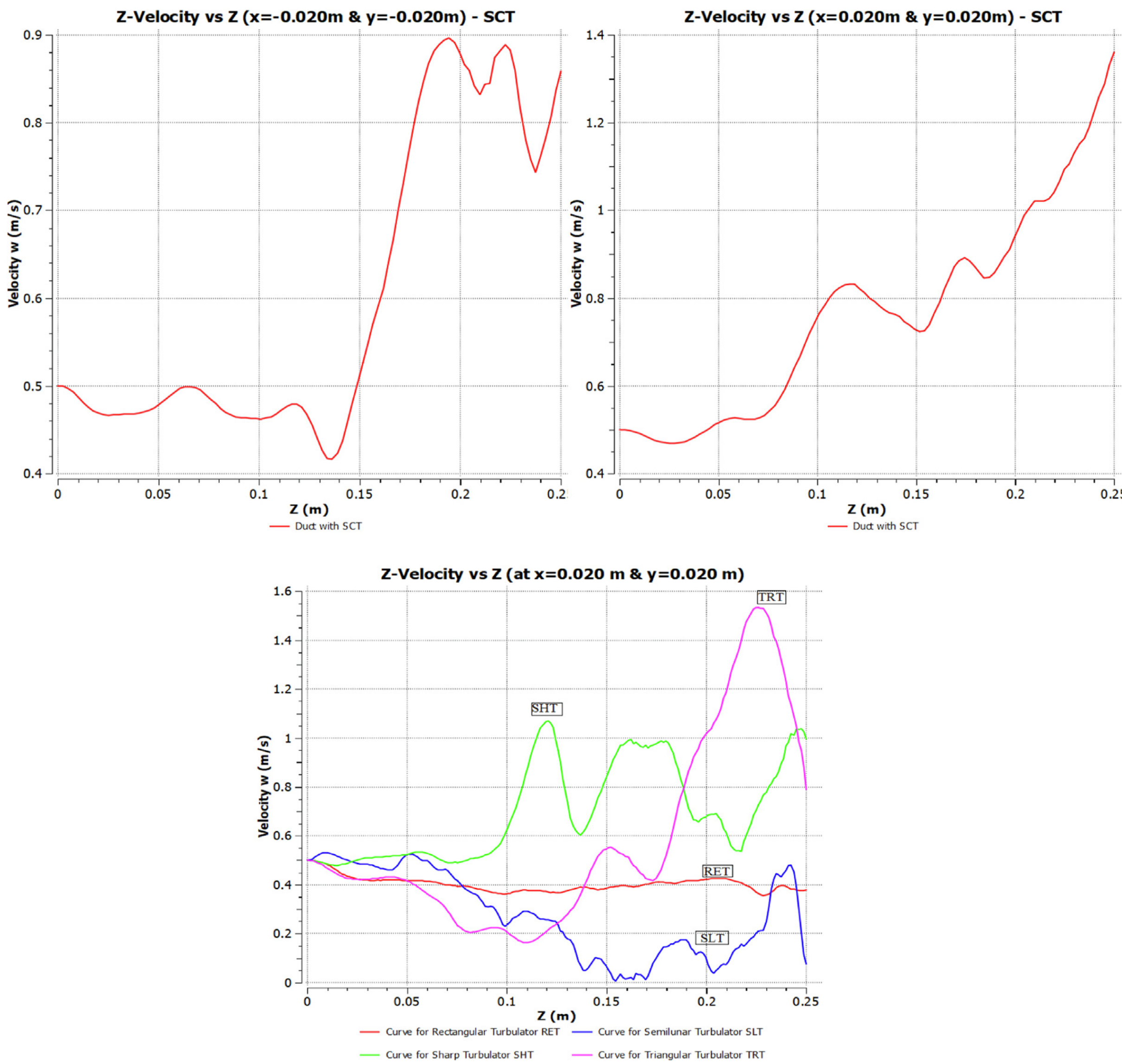

Fig. 7 Variations of the z- component of the fluid velocity according to the duct length equipped with turbulators SCT,SHT, SLT, RET and TRT.

Table 5 Investigating fluid velocity changes along the z direction along the channel with various meshes and turbulators.

Z-Velocity (m/s) at x = 20 mm & y = 20 mm										
Duct Length	Z = 15 mm	Z = 35 mm	Z = 60 mm	Z = 90 mm	Z = 125 mm	Z = 170 mm	Z = 190 mm	Z = 200 mm	Z = 220 mm	Z = 230 mm
SCT	0.4808427	0.4764975	0.5262976	0.6624363	0.8107759	0.8776369	0.8607545	0.9410065	1.0401628	1.1313576
TRT	0.4420641	0.4266883	0.3622311	0.2211424	0.2374302	0.4252107	0.8304998	1.0265337	1.4758666	1.5105292
RET	0.4566293	0.4183377	0.4139468	0.3741018	0.3678228	0.4013302	0.4168566	0.4221385	0.3975757	0.3591142
SHT	0.4793611	0.5123214	0.5285342	0.5239466	0.9946331	0.9701384	0.7482281	0.6773127	0.5998974	0.7787294
SLT	0.5156377	0.472902	0.4985212	0.3084998	0.2499423	0.0116403	0.1751721	0.104685	0.1586193	0.2517445

for this parameter, all the ratios are greater than unity during the passage inside the duct containing the turbulator has been reduced to a small amount. The greatest decrease in this ratio is related to it has been SLT (37.47 %), TRT (11.15 %), SCT (3.42 %), SHT (2.77 %), and RET (1.87 %). Another important quantity is the fluid pressure drop when passing through a duct equipped with a turbulator. In most industries, this quantity is very important, because it affects the capacity and power of pumps and compressors feeding the working fluid accordingly. Looking at Fig. 12, even though the fluid pressure drop is decreasing while passing through all the ducts equipped with turbulator and the geometry of the SLT turbulator is optimal in turbulent flow, the amount of drop in the pressure has been relatively high. The pressure drop of the operating fluid in

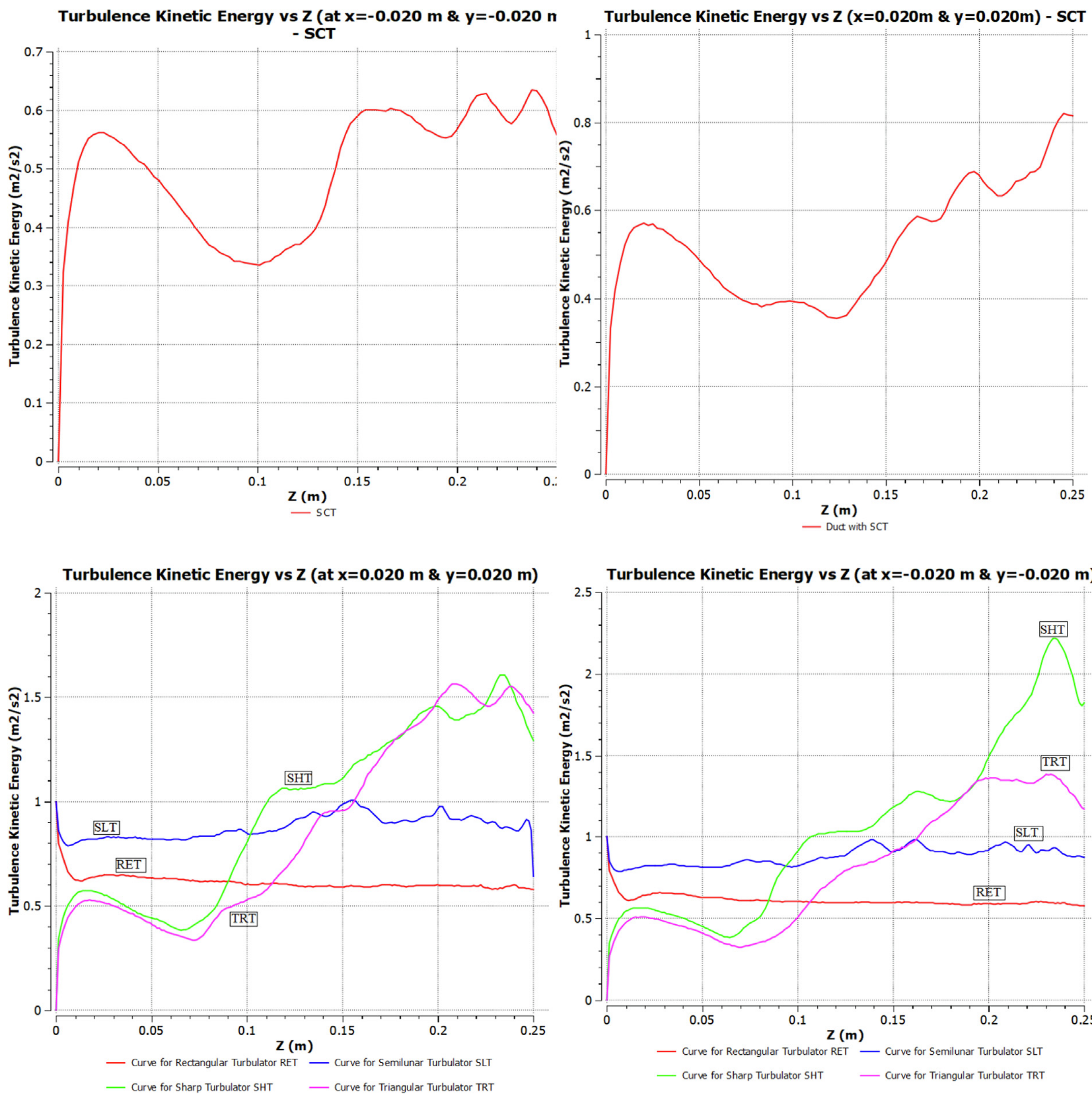

Fig. 8 Variations of the kinematic energy of the turbulent flow according to the duct length equipped with turbulators SCT,SHT, SLT, RET and TRT.

Table 6 Investigating Turbulence Kinetic Energy changes along the channel with various meshes and turbulators.

Turbulence Kinetic Energy (m^2/s^2) at x = 20 mm & y = 20 mm												
Duct Length	Z = 10 mm	Z = 15 mm	Z = 20 mm	Z = 35 mm	Z = 60 mm	Z = 90 mm	Z = 125 mm	Z = 170 mm	Z = 190 mm	Z = 200 mm	Z = 220 mm	Z = 230 mm
SCT	0.5209143	0.5606642	0.5707757	0.5421158	0.4409704	0.3900012	0.3558741	0.5811265	0.6626357	0.6798534	0.6663003	0.6894653
TRT	0.4962256	0.5228246	0.5235816	0.4789942	0.3693393	0.4905936	0.7432925	1.207455	1.3749714	1.4820344	1.4954436	1.4728773
RET	0.6239799	0.6275234	0.6379178	0.6477202	0.6295458	0.6175808	0.5965984	0.5976648	0.595899	0.5995753	0.5954037	0.5814883
SHT	0.5549411	0.5724523	0.5670731	0.5053927	0.4019676	0.6279258	1.0592388	1.2502322	1.4155036	1.4567449	1.4297829	1.5650544
SLT	0.8001638	0.8169736	0.8210825	0.8284204	0.8161129	0.8607814	0.9146856	0.9111931	0.9127557	0.9626371	0.926451	0.9000324

other ducts containing the turbulator is respectively from SLT (51.64 %), TRT (43.26 %), SCT (22.19 %), SHT (17.83 %), and RET (9.61 %).

In conclusion, based on the investigations carried out and the calculations made, in order of comparison, turbulators SLT and then TRT compared to other turbulators (TRT, SHT, RET) It has the highest Nusselt number And in the Reynolds numbers in the turbulent flow regime, they have the greatest reduction in the friction coefficient. Whereas that the most pressure drop has occurred in these two types of tur-

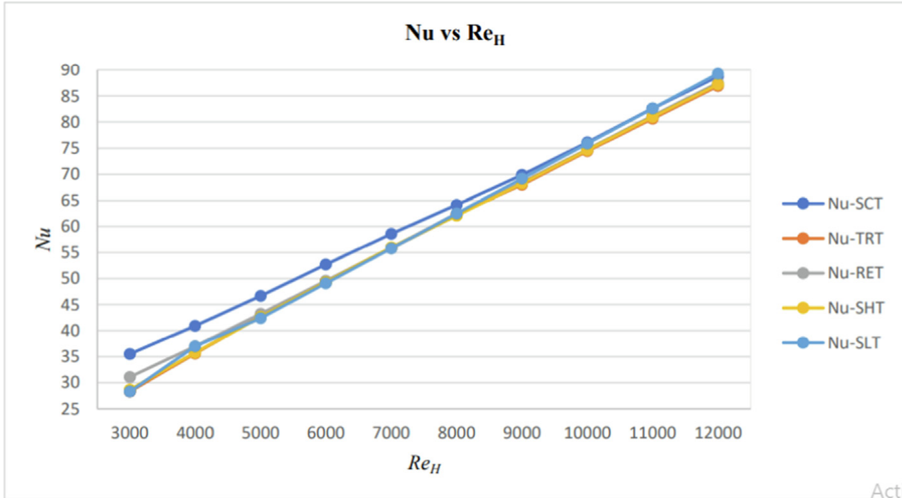

Fig. 9 Changes of Nusselt number in terms of Reynolds number for ducts equipped with 5 turbulators.

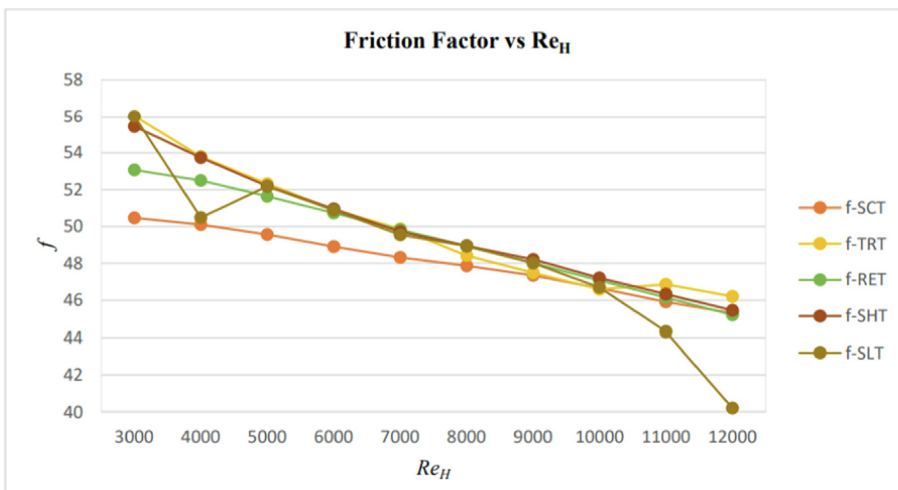

Fig. 10 Changes of friction factor in terms of Reynolds number for ducts equipped with 5 turbulators.

bulators. On the other hand, the efficiency of heat transfer in these two types turbulator is more than other turbulators, and in terms of TKE values, it is in a more suitable position.

Dynamic pressure is the kinetic strength consistent with unit quantity of fluid. Dynamic pressure is one of the terms in Bernoulli's condition and can be inferred from energy preservation in moving liquids. Dynamic pressure is the pressure created by the movement of liquids. The above figures show the changes in the values of the fluid dynamic pressure parameter around the types of turbulators with different sections. The most pressure changes have occurred around the flow in the oblong shaped turbulator, so that the pressure parameter is maximum in the middle of the turbulator. Also, the highest and lowest values of the dynamic pressure of the working fluid, comparatively, among the ducts equipped with turbulator, respectively, are related to SLT ($P_{Dyn.max.}$) = 1866.15 at Z = 15 mm, $P_{Dyn.min.}$) = 494.66 at Z = 230 mm) and RET ($P_{Dyn.max.}$) = 202.70 at Z = 90 mm, $P_{Dyn.min.}$) = 42.62 at Z = 190 mm).

Turbulence kinetic energy measures the strength of turbulence in a flow. Turbulence kinetic energy (TKE) is one of the biggest essential quantities in micrometeorology as it is a measure of the strength of turbulence. This is directly linked to the transport of momentum, heat and moisture across the boundary layer. As can be seen in both coordinates, the turbulent flow kinematic energy (TKE) in the semi-cylindrical turbulator (SCT) was almost similar and had a current difference, and also in the SLT and RET turbulators, it was almost with-

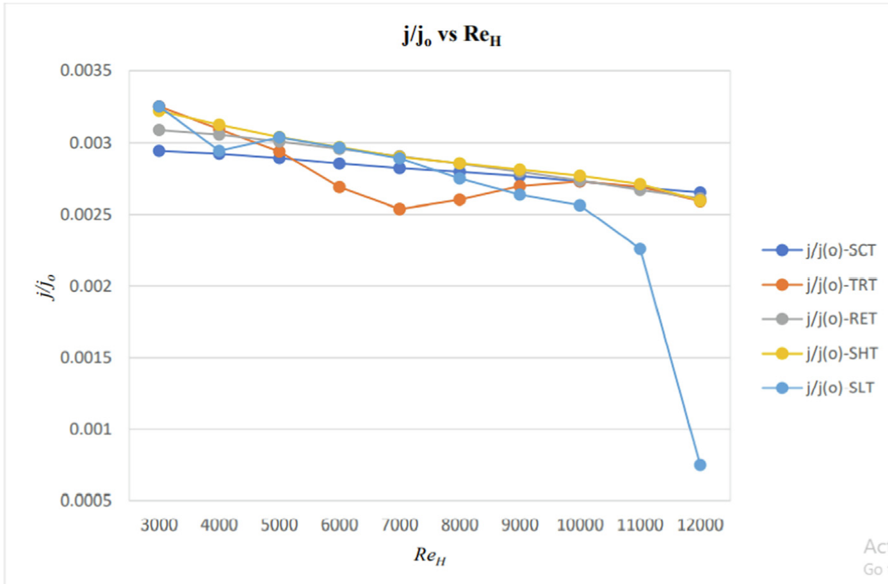

Fig. 11 Changes of Colburn coefficient in terms of Reynolds number for ducts equipped with 5 turbulators.

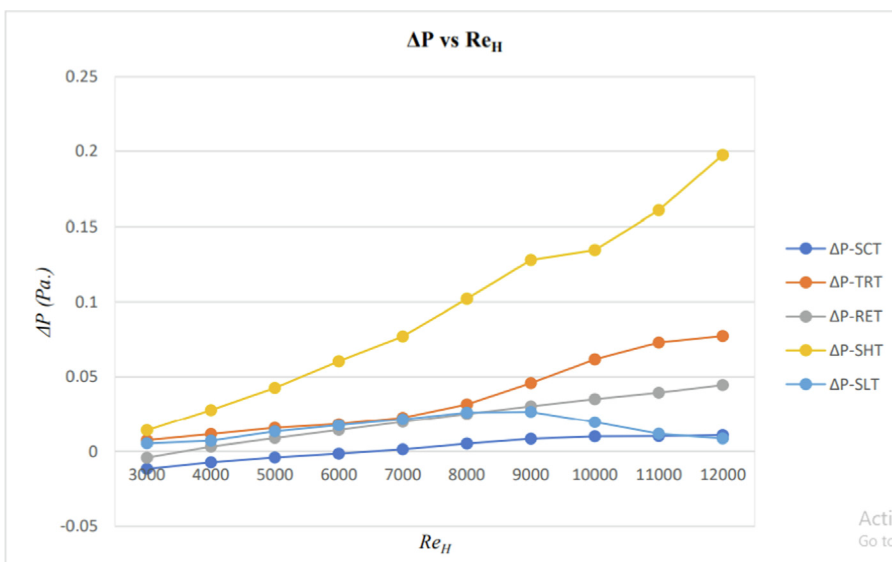

Fig. 12 Changes of pressure drop in terms of Reynolds number for ducts equipped with 5 turbulators.

out ups and downs, and within a certain range. They fluctuated a little, but SHT and TRT turbulators, had the most fluctuation and had the maximum value (Figs. 13–14).

5. Conclusion

The principal moot point in this investigation is heat removal from surfaces with high heat flux, which is the use of tabulators and parts with a particular geometry, it has been chosen as a solution to this moot point. The basic hypothesis in this investigation is to increase fluid heat transfer by increasing turbulence and increasing heat transfer by increasing the plane of heat transfer and establishing a vortex flow. The fundamental idea of this investigation is the simultaneous use of a turbulator (in order to increase turbulence and provide more effective heat transmission), and increasing the contact surface (through the installation of parts with special geometry) which can be obtained from different turbulator used other geometries.

- An increase in the value of the Reynolds number causes an increase in the value of the Nusselt number and a decrease in the fluid friction coefficient.
- Number a Nusselt greater than unity indicates a higher displacement heat transfer, and the larger this number is, the transfer more heat transfer is done.

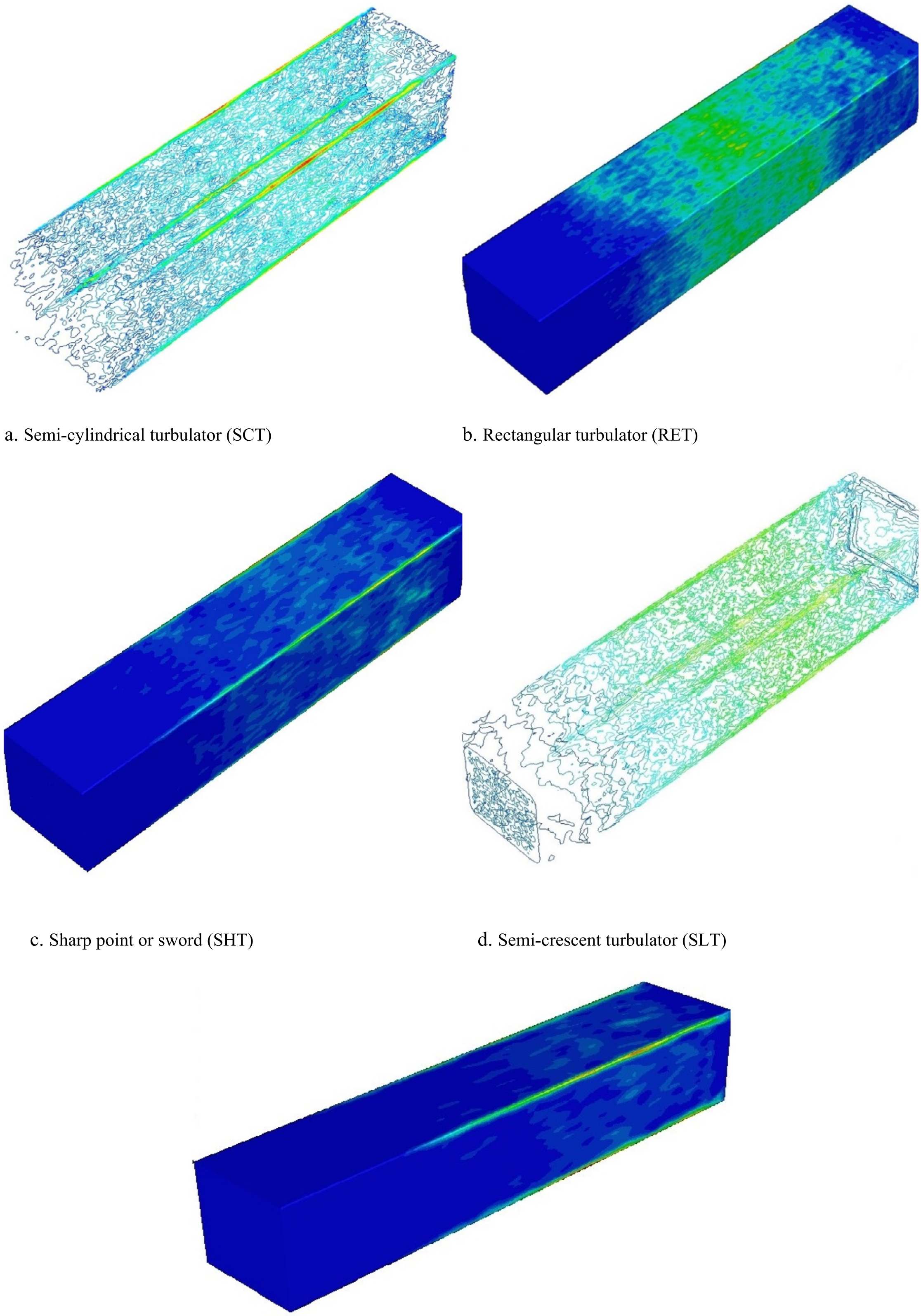

a. Semi-cylindrical turbulator (SCT)
b. Rectangular turbulator (RET)
c. Sharp point or sword (SHT)
d. Semi-crescent turbulator (SLT)
e. Semi-triangular turbulator (TRT)

Fig. 13 Changes of dynamic pressure around the ducts equipped with 5 turbulators.

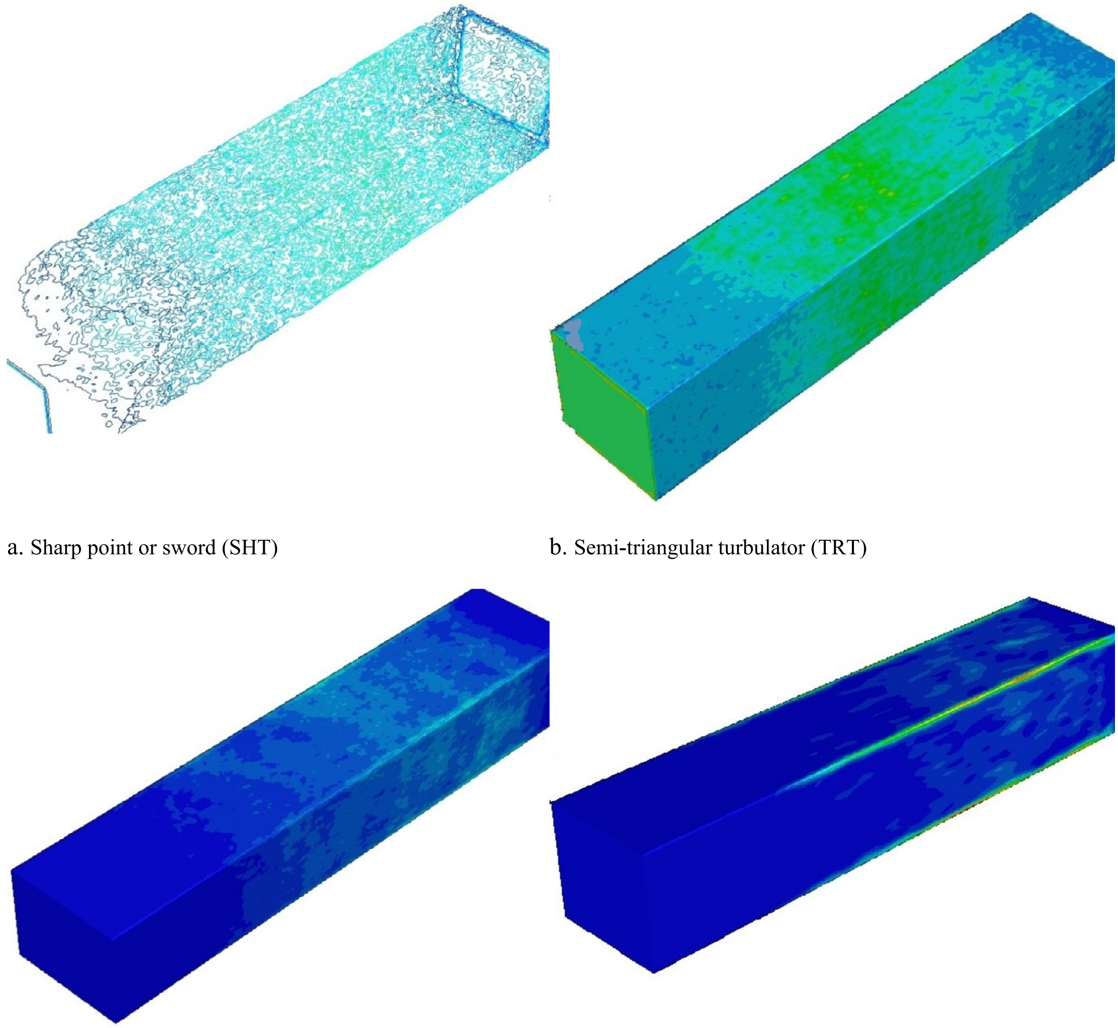

a. Sharp point or sword (SHT) b. Semi-triangular turbulator (TRT)

c. Semi-cylindrical turbulator (SCT) d. Rectangular turbulator (RET)

Fig. 14 Changes of turbulent kinetic energy the ducts equipped with 4 turbulators.

- Turbulators SLT and then TRT compared to other turbulators (TRT, SHT, RET) It has the highest Nusselt number and in the Reynolds numbers in the turbulent flow regime, they have the greatest reduction in the friction coefficient.
- Among the suggestions to continue the main topic of this article, we can mention the addition of a series of equations with magnetism parameter next to the types of turbulators, so that the produced magnetic flux affects the fluid velocity and Nusselt number.

Declaration of Competing Interest

The authors declare that they have no known competing financial interests or personal relationships that could have appeared to influence the work reported in this paper, and No funds have been given to them.

References

[1] S. Shaheen et al, A case study of heat transmission in a Williamson fluid flow through a ciliated porous channel: a semi-numerical approach, Case Stud. Therm. Eng. 41 (2023) 102523.

[2] Bég, O. Anwar, et al. Numerical solutions for axisymmetric non-Newtonian stagnation enrobing flow, heat, and mass transfer with application to cylindrical pipe coating dynamics. *Computational Thermal Sciences: An International Journal* 12.1 (2020).

[3] Al-Kouz, Weal, et al. Heat transfer and entropy generation analysis of water-Fe3O4/CNT hybrid magnetic nanofluid flow in a trapezoidal wavy enclosure containing porous media with the Galerkin finite element method. *The European Physical Journal Plus* 136.11 (2021): 1184.

[4] W. Jamshed et al, Thermal characterization of coolant Maxwell type nanofluid flowing in parabolic trough solar collector (PTSC) used inside solar powered ship application, Coatings 11 (12) (2021) 1552.

[5] Bég, O. Anwar, et al. Experimental study of improved rheology and lubricity of drilling fluids enhanced with nano-particles. *Applied Nanoscience* 8 (2018): 1069–1090.
[6] A. Boonloi, W. Jedsadaratanachai, Thermohydraulic performance improvement in heat exchanger square duct inserted with 45 inclined square ring, Model. Simul. Eng. (2020).
[7] A. Verma, M. Kumar, A.K. Patil, Enhanced heat transfer and frictional losses in heat exchanger tube with modified helical coiled inserts, Heat Mass Transf. 54 (10) (2018) 3137–3150.
[8] Z. Azizi, V. Rostampour, S. Jafarmadar, S. Khorasani, B. Abdzadeh, Investigating the effect of strip turbulator pitch on heat transfer and pressure drop of two-phase water-air flow, in: The 28th Annual International Conference of the Iranian Society of Mechanical Engineers, https://civilica.com/doc/1029314.
[9] Z. Xu et al, The characteristics of heat transfer and flow resistance in a rectangular channel with vortex generators, Int. J. Heat Mass Transf. 116 (2018) 61–72.
[10] H. Hosseini et al, Development in household water heaters by replacing the shell and tube heat exchangers by inclined flat ones having rectangular fins, Case Stud. Therm. Eng. 28 (2021) 101490.
[11] M. Alizadeh et al, An analysis of latent heat thermal energy storage in a hexagonal triplex-tube unit with curve shape fin and CNTs, Case Stud. Therm. Eng. 36 (2022) 102241.
[12] Zhao, Jinguo, et al., Hydro-thermal and economic analyses of the air/water two-phase flow in a double tube heat exchanger equipped with wavy strip turbulator, Case Stud. Therm. Eng. 37 (2022) 102260, doi: 10.1016/j.csite.2022.102260.
[13] F. Aldawi, Proposing the employment of spring-wire turbulator for flat spiral tubes utilized in solar ponds, experimental study, Case Stud. Therm. Eng. (2022) 102180.
[14] B. Shaker et al, CFD analysis of Al2O3-syltherm oil nanofluid on parabolic trough solar collector with a new flange-shaped turbulator model, Theor. Appl. Mech. Lett. 12 (2) (2022) 100323.
[15] S.M. Seyyedi et al., Investigation of entropy generation in a square inclined cavity using control volume finite element method with aided quadratic Lagrange interpolation functions, Int. Commun. Heat Mass Transf. 110 (2020) 104398, doi: 10.1016/j.icheatmasstransfer.2019.104398.
[16] H. Nabi et al., Increasing heat transfer in flat plate solar collectors using various forms of turbulence-inducing elements and CNTs-CuO hybrid nanofluids, Case Stud. Therm. Eng. 33 (2022) 101909, doi: 10.1016/j.csite.2022.101909.
[17] K. Hosseinzadeh et al, Experimental and numerical study for the effect of aqueous solution on heat transfer characteristics of two phase close thermosyphon, Int. Commun. Heat Mass Transfer 135 (2022) 106129.
[18] M.R. Zangooee, K. Hosseinzadeh, D.D. Ganji, Hydrothermal analysis of MHD nanofluid (TiO2-GO) flow between two radiative stretchable rotating disks using AGM, Case Stud. Therm. Eng. 14 (2019) 100460, doi: 10.1016/j.csite.2019.100460.
[19] M.R. Zangooee, K.h. Hosseinzadeh, D.D. Ganji, Hydrothermal analysis of hybrid nanofluid flow on a vertical plate by considering slip condition, Theor. Appl. Mech. Lett. (2022) 100357.
[20] R. Fathollahi, et al., Analyzing the effect of radiation on the unsteady 2D MHD Al2O3-water flow through parallel squeezing sheets by AGM and HPM, Alex. Eng. J. (2022), Volume 69, 15 April 2023, Pages 207–219.
[21] K. Hosseinzadeh et al, Solidification enhancement in triplex thermal energy storage system via triplets fins configuration and hybrid nanoparticles, J. Storage Mater. 34 (2021) 102177.